



Theoretical background and experimental measurements of human brain noise intensity in perception of ambiguous images



Anastasiya E. Runnova^{a,b}, Alexander E. Hramov^{a,b,*}, Vadim V. Grubov^a,
Alexey A. Koronovskii^{b,a}, Maria K. Kurovskaya^{b,a}, Alexander N. Pisarchik^{a,c,d}

^a Research and Education Center 'Nonlinear Dynamics of Complex Systems', Yuri Gagarin State Technical University of Saratov, Politehnicheskaya, 77, Saratov, 410054, Russia

^b Saratov State University, Astrakhanskaya, 83, Saratov, 410012, Russia

^c Center for Biomedical Technology, Technical University of Madrid, Campus Montegancedo, 28223 Pozuelo de Alarcon, Madrid, Spain

^d Centro de Investigaciones en Optica, Loma del Bosque 115, Lomas del Campestre, 37150 Leon, Guanajuato, Mexico

ARTICLE INFO

Article history:

Received 5 June 2016

Revised 11 October 2016

Accepted 2 November 2016

Keywords:

Brain

Noise

Ambiguous image

Multistability

ABSTRACT

We propose a theoretical approach associated with an experimental technique to quantitatively characterize cognitive brain activity in the perception of ambiguous images. Based on the developed theoretical background and the obtained experimental data, we introduce the concept of effective noise intensity characterizing cognitive brain activity and propose the experimental technique for its measurement. The developed theory, using the methods of statistical physics, provides a solid experimentally approved basis for further understanding of brain functionality. The rather simple way to measure the proposed quantitative characteristic of the brain activity related to the interpretation of ambiguous images will hopefully become a powerful tool for physicists, physiologists and medics. Our theoretical and experimental findings are in excellent agreement with each other.

© 2016 Elsevier Ltd. All rights reserved.

1. Introduction

The brain is one of the most sophisticated and enigmatic objects of comprehensive study attracting the burning interest of a broad scientific community [1–9]. Due to its immense importance and complexity, the brain research requires the combined efforts of scientists from diverse areas, including psychology, neurophysiology, medicine, physics, mathematics, and nonlinear dynamics. The multidisciplinary approach providing insight into the mysteries of the brain and a deeper understanding of mechanisms underlying its dynamics, opens promising opportunities for humanity with applications in medicine and neurotechnology in the nearest future.

The perception of ambiguous images [10,11] is just one very exciting task among an enormous number of open problems which appeared during recent intensive brain studies. Visual perception was often studied through perceptual alternations while observing ambiguous images [12–16], although perceptual alternations were also described for other modalities [17–19]. In addition, this phenomenon is tightly connected with the problem of categorical per-

ception [20] (including non-human primates [21,22]). Even though the underlying mechanism of image recognition is not yet well understood, the metastable visual perception is known to involve a distributed network of occipital, parietal and frontal cortical areas [23,24]. The generally accepted concept that throws light on this phenomenon includes noise [25–28] inherent to neural brain cells activity originated from random neuron spikes [29].

Internal brain noise seems to play a crucial role in brain dynamics related to the perception activity [25–27] and other brain functions [30–33]. Different manifestations of stochastic processes in the brain, including the perception of ambiguous images, were extensively studied in terms of simple stochastic processes like the Wiener process [34–37] from the viewpoint of statistical properties [26–28,38,39]. The development of methods for quantitative measurement of the brain's stochastic properties can open up plenty of new opportunities for the study of the brain functionality and a diagnosis of brain pathologies. In the present work, we develop the quantitative theory and propose the experimental technique for measuring brain noise intensity related to the perception of ambiguous images. We carry out psychological experiments which confirm our theoretical findings and proposed methodological approach.

* Corresponding author.

E-mail address: hramovae@gmail.com (A.E. Hramov).

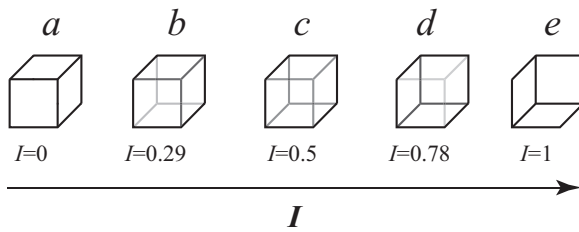


Fig. 1. Examples of distinct Necker cube images with different wireframe contrasts characterized by control parameter I .

2. Experimental study description

The experimental studies were performed in accordance with the ethical standards [40] and approved by the local research ethics committee of Saratov State Technical University. Twenty healthy subjects from a group of unpaid volunteers, male and female, between the ages of 20 and 45 with a normal or corrected-to-normal visual acuity participated in the experiments. All persons have provided informed consent before participating in the experiment. As an ambiguous image, we used the Necker cube [41]. The contrast of the three middle lines centered in the left middle corner, $I \in [0, 1]$, was used as a control parameter. The values $I = 1$ and $I = 0$ correspond, respectively, to 0 (black) and 255 (white) pixels' luminance of the middle lines, using the 8-bit grayscale palette for visual stimulus presentation. Therefore, we can define contrast parameter as $I = y/255$ where y is the brightness level of the middle lines in used 8-bit grayscale palette. The contrast of the three middle lines centered in the right middle corner was set to $(1 - I)$, and the contrast of the six visible outer cube edges was fixed to 1.

During the experiment $N = 16$ Necker cube images with different wireframe contrasts, i.e. with different values of the control parameter I (Fig. 1), were repeatedly presented to a person in a random sequence; each cube drawn by black lines was placed in the middle of a computer screen on a white background. All participants were well aware about the two possible orientations of the Necker cube, and both orientations were seen by all of them. All participants were instructed to press either the left or the right key on the control panel according to their first visual impression (left-oriented cube (Fig. 1(a)) or right-oriented cube (Fig. 1(e))). Both the image presentation and the recording of personal responses were accomplished with the help of Electroencephalograph-recorder Encephalan-EEGR-19/26 (Medicom MTD). To demonstrate the grayscale stimulus we used a 24" BenQ LCD monitor with the spatial resolution 1920×1080 pixels and refresh rate of 60 Hz. The subject was located at a distance of 70–80 cm from the monitor with visual angle approximately equal to 0.25 rad. The overall observation time of each experiment was 32 min, each Necker cube with the fixed control parameter I_j ($j = 1, \dots, N$) being shown randomly $K = 47$ times. In other words, during one experiment $M = N \times K = 752$ stimuli were presented to the observer. The schematic representation of the experiment paradigm is given in Fig. 2.

The choice of the durations of stimuli presentations, τ_i , as well as lengths of intervals between stimuli, s_i (see Fig. 2), plays the important role. Since the stimuli are presented to the observer intermittently, the effect of the stabilization of visual perception can take place [42]. The underlying mechanism of this stabilization effect is not clear yet (although there are known some model-based approaches, see, e.g. [43]), but obviously, that this effect consisting in persisting the visual perception between subsequent presentations of two ambiguous images can potentially affect the results.

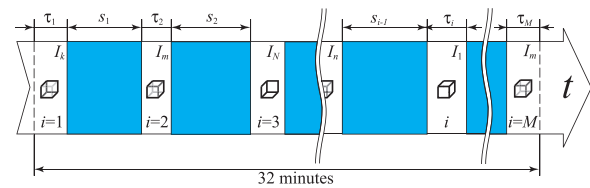


Fig. 2. The schematic representation of the experiment paradigm. The white rectangles correspond to the epochs with durations τ_i ($\tau_i \sim 0.5\text{--}0.7$ s, $i = 1, 2, \dots, M$). Within each epoch of the stimulus presentation the randomly selected Necker cube with one of the control parameter values I_j ($j = 1, \dots, N$) is shown to the observer. Time intervals (with durations $s_i \sim 1.5\text{--}2.0$ s when the different abstract pictures are demonstrated) between stimuli presentations are marked by dark rectangles. Two vertical dashed lines correspond to the start and finish of experiment, respectively. The total length of the experiment is 32 min when $M = 752$ times the Necker cube images are presented to the observer, with each of N Necker cubes (with the fixed control parameter value I_j) being shown exactly $K = 47$ times.

Therefore, the durations τ_i and s_i should be chosen in such a way to avoid the stabilization effect.

The mean duration of a visual percept is known to vary from one second to several minutes depending on each observer and stimulus conditions (e.g., [44]), whereas the mean response times are rather consistent and vary only by a few hundred milliseconds (see, e.g. [45]). The most common experimental length for each percept of the Necker cube was found to be approximately 1 s [28]. Therefore, to fix the first impression of the person and avoid switches between two possible percepts the image exhibition was limited to $\tau \sim 0.5\text{--}0.7$ s. This length of the stimuli presentation allows also reducing the stabilization effect [42] described above. Indeed, the probability of a configuration persisting until the subsequent presentation is known to be highly dependent on how long it was seen before the stimulus was removed [42]. Only when a perceptual configuration was seen consistently for the relatively long time before the stimulus disappearance, there is a high probability that it would persist to the next stimulus presentation. For the Necker cube this required time of the consistent observation is known to be about 1 s [42], and, therefore, taking the length of the stimulus exhibition τ below this value, we reduce the “memory” effect. The random sequence of the Necker cubes with the different values of the control parameter, I (see Fig. 2), also prevents the appearance of the perception stabilization. Lastly, to draw away the observer's attention and make the perception of the next Necker cube image independent of the previous one, the different abstract pictures were exhibited for about $s \sim 1.5\text{--}2.0$ s between subsequent demonstrations of different Necker cube images.

For each value I_j of the control parameter I the probability $P_l(I_j)$ of the left-oriented cube (the left key choice) was calculated as

$$P_l(I_j) = \frac{l(I_j)}{l(I_j) + r(I_j)}, \quad (1)$$

where $l(I_j)$ and $r(I_j)$ are the numbers of clicks on the left and right keys, respectively, for the j -th Necker cube with the value I_j of the control parameter.

3. Theoretical approach

The probability of a subject to perceive the left-oriented image of the Necker cube $P_l(I)$ is, in fact, a psychometric function actively studied in psychophysics [46–48]. In the framework of classical approach, different empirical functions (such as Cumulative, Normal, Logistic, Weibull, Gumbel, etc.) are used to model experimentally obtained psychometric functions, with control parameters (first of all, threshold and slope) fitted with the help of different methods, e.g., maximum likelihood criterion or Bayesian criterion [47,49]. Although such an approach allows the quantitative description of the

dependence of an observer’s performance on some physical parameters of visual stimulus, this kind of description is mainly empirical, tangling different aspects and mechanisms of the brain activity.

Contrary to the traditional approach [46,47,49], in our study we mainly focus on the theoretical and quantitative description as well as the experimental measurement of the concrete relevant factor of the brain activity, namely, the noise intensity characterizing stochastic processes in the brain. Based on the methods of statistical physics, we develop a theory which helps us to derive the analytical (not empirical) expression of the experimental data and measure the brain noise intensity.

In previous studies [25,27,50,51] different possible interpretations of ambiguous images were attributed to the competition between neuronal populations. The alternation between two possible interpretations of an ambiguous image, such as the Necker cube [28] and other images (see, e.g., [27,39]) indicates that the system is close to the cusp catastrophe [52]. It is well known that absolutely all systems in the vicinity of the cusp catastrophe are described by the dimensionless potential energy function with two local minima x_l, r :

$$U(x) = \frac{a_4 x^4}{4} + \frac{a_3 x^3}{3} + \frac{a_2 x^2}{2} + a_1 x. \tag{2}$$

In the case of the Necker cube this corresponds to the left- and right-oriented perception states. In the context of the considered problem, the neuronal population dimensionless firing rate x is qualitatively described by the ordinary differential equation

$$\dot{x} = -U'(x) + \xi(t), \tag{3}$$

where $\xi(t)$ is supposed to be zero mean δ -correlated Gaussian noise [$\langle \xi(t) \rangle = 0$, $\langle \xi(t) \xi(t_1) \rangle = D \delta(t - t_1)$], D is the noise intensity, $\delta(\cdot)$ is the Dirac δ -function. Recent studies of the stochastic model Eq. (3) have demonstrated a very good qualitative agreement between numerical and experimental results [14,27], although the problem of the direct quantitative description of the stochastic brain processes has not been solved hitherto.

Generally, the profile of the perception energy function $U(x)$ may vary for each individual. Moreover, it may even change from time to time for the same person depending on his/her health, mood, tiredness, adaptation ability, etc. Therefore, coefficients a_i are expected to vary for each person and experiment. Fortunately, by changing variables the profiles Eq. (2) with different coefficients a_i can be reduced to the universal form [52]

$$U(x) = \frac{x^4}{4} - \frac{x^2}{2} + bx \tag{4}$$

to be used in Eq. (3). Indeed, substituting new variable z for x ($x = \delta z + \Delta$, where $\delta = \sqrt{a_3^2 - 3a_2 a_4} / (\sqrt{3} a_4)$ and $\Delta = -a_3 / (3a_4)$) in Eq. (2) and neglecting the constant term (which is insufficient since the derivative of the potential function is used in Eq. (3)), one can obtain the potential energy function in the form

$$U(z) = \gamma \left(\frac{z^4}{4} - \frac{z^2}{2} + bz \right), \tag{5}$$

where

$$b = \frac{2a_3^3 - 9a_2 a_3 a_4 + 27a_1 a_4^2}{3\sqrt{3}\sqrt{(a_3^2 - 3a_2 a_4)^2}} \quad \text{and} \quad \gamma = \frac{(a_3^2 - 3a_2 a_4)^2}{9a_4^3}. \tag{6}$$

The multiplier γ , in turn, may be eliminated from the consideration with the help of the time axes scaling $\tau = \gamma t$. One can see, that after these transformations of variables the obtained potential energy function (5) coincides with Eq. (4) up to notations. Since the noise intensity is also changed with substitution of the variables ($D_{new} = D/\gamma^2$), we propose to consider and measure the intensity of the effective noise related to the universal form of

the perception energy Eq. (4). Therefore, starting from this point, we assume that the bistable visual perception is governed by the stochastic model Eq. (3) with the energy function given by Eq. (4) with $b = \Delta I/\alpha$, where ΔI is the deviation of the Necker cube parameter from the symmetrical case and α is unknown scaling coefficient determined by individual particularities of the bistable perception energy function.

The stochastic term in Eq. (3) results in the stochastic differential equation

$$dX = -U'(x) dt + dW, \tag{7}$$

where $X(t)$ describes a stochastic process, $W(t)$ supposed to be a one-dimensional Wiener process which may be solved using the Fokker-Plank equation

$$\frac{\partial \rho_X(x, t)}{\partial t} = \frac{\partial}{\partial x} [U'(x) \rho_X(x, t)] + \frac{D}{2} \frac{\partial^2 \rho_X(x, t)}{\partial x^2} \tag{8}$$

written for probability density $\rho(x, t)$ of the stochastic process $X(t)$. The stationary probability density $\rho(x)$ being the solution of Eq. (8) does not depend on time t , and, therefore, Fokker-Plank equation Eq. (8) may be reduced to the ordinary differential equation

$$\frac{d}{dx} [U'(x) \rho(x)] + \frac{D}{2} \frac{d^2 \rho(x)}{dx^2} = 0. \tag{9}$$

Obtained equation Eq. (9) is equivalent to

$$\rho'(x) + \frac{2}{D} U'(x) \rho(x) - C = 0, \tag{10}$$

where C is unknown constant. To solve the inhomogeneous ordinary differential equation of the first order Eq. (10) we first consider the homogeneous ordinary differential equation

$$\rho'(x) + \frac{2}{D} U'(x) \rho(x) = 0, \tag{11}$$

which solution is

$$\rho(x) = B e^{-\frac{2}{D} U(x)}, \tag{12}$$

where B is constant. The solution of the inhomogeneous ordinary differential equation Eq. (10) is known to have the form

$$\rho(x) = B(x) e^{-\frac{2}{D} U(x)}. \tag{13}$$

Having substituted Eq. (13) for $\rho(x)$ in Eq. (10) one can obtain the differential equation for the unknown function $B(x)$ as

$$B'(x) = C e^{\frac{2}{D} U(x)}, \tag{14}$$

which solution may be written in the form

$$B(x) = C \int_0^x e^{\frac{2}{D} U(z)} dz + A, \tag{15}$$

where A is some constant. Finally, taking into account Eqs. (12) and (15) we obtain the general form of the stationary probability density $\rho(x)$ being the solution of Fokker-Plank Eq. (8) as

$$\rho(x) = e^{-\frac{2U(x)}{D}} \left[A + C \int_0^x e^{\frac{2U(z)}{D}} dz \right]. \tag{16}$$

Having found the constant C from the extremum condition

$$\rho'(x_{l,r}) = C = 0 \tag{17}$$

we obtain the final form for the stationary probability density function

$$\rho(x) = A \exp \left(-\frac{2U(x)}{D} \right), \tag{18}$$

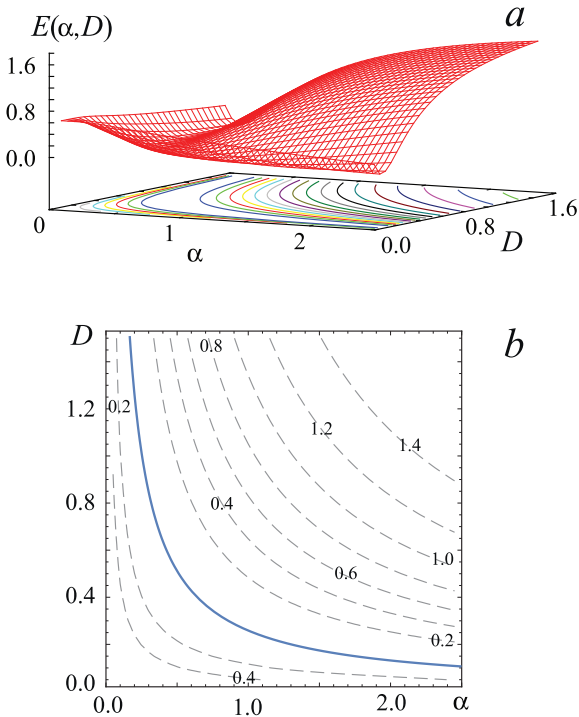


Fig. 3. (a) The surface of error values $E(\alpha, D)$ of the least square method calculated for observer #13 and (b) the contour plot corresponding to this surface. The bold (blue) solid line in (b) represents the curve $\alpha D = 0.255$ corresponding to the minimum error $E_{\min} = 10^{-2}$.

where A is determined by the normalization condition

$$\int_{-\infty}^{+\infty} \rho(x) dx = 1. \tag{19}$$

As a consequence, the theoretical probability for the person to perceive the left-oriented cube, \hat{P}_l , can be found as

$$\hat{P}_l = \int_{-\infty}^0 \rho(x) dx, \tag{20}$$

where \hat{P}_l depends on three control parameters, namely, ΔI , α and D , i.e., $\hat{P}_l = \hat{P}_l(\Delta I, \alpha, D)$.

By varying the quantity ΔI , while two other control parameters, α and D , are fixed, one can obtain the theoretical curve $\hat{P}_l(\Delta I, \alpha, D)$ corresponding to the experimental data which, in turn, may be also considered as dependent on the deviation of the Necker cube parameter from the symmetrical case, i.e., $P_l = P_l(\Delta I)$. The values of two other parameters, α and D , can be found with the help of the least square technique [53] for the minimum error value

$$E(\alpha, D) = \sum_{j=1}^N [P_l(\Delta I_j) - \hat{P}_l(\Delta I_j, \alpha, D)]^2. \tag{21}$$

4. Results

The typical surface of error $E(\alpha, D)$ calculated by using the least square method is shown in Fig. 3(a), whereas the contour plot corresponding to this surface is given in Fig. 3(b). One can clearly see that there is the curve of the minimal error E_{\min} for which the best coincidence of the theoretical and experimental points occurs. This curve found empirically is described by the following approximate relation [see Fig. 3(b)]

$$\alpha D = D_p = \text{const}. \tag{22}$$

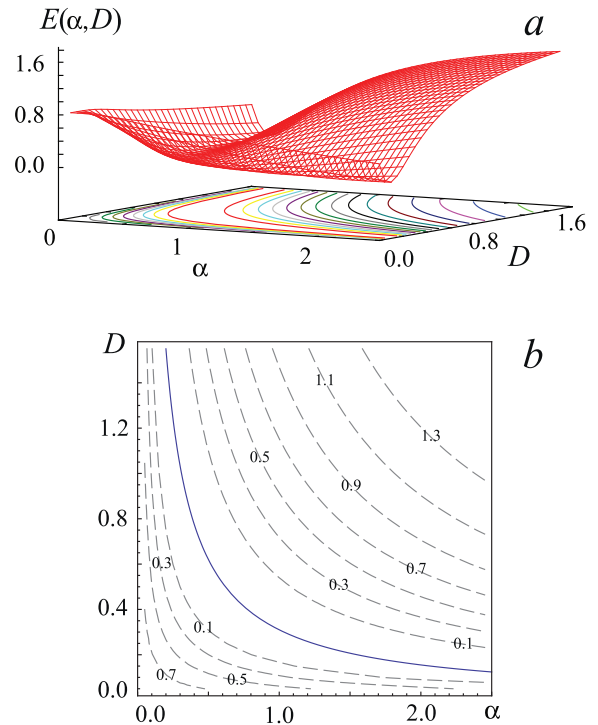


Fig. 4. (a) The surface of error values $E(\alpha, D)$ of the least square method calculated for observer #1 and (b) the contour plot corresponding to this surface. The bold (blue) solid line in (b) represents the curve $\alpha D = D_p = 0.31$ corresponding to the minimum error $E_{\min} = 0.026$.

Table 1

The values of the noise intensity D_p measured experimentally and the minimum error E_{\min} characterizing the deviation of the experimentally obtained P_l from the theoretical predicted \hat{P}_l .

#	D_p	E_{\min}	#	D_p	E_{\min}	#	D_p	E_{\min}
1	0.310	0.026	8	0.205	0.085	15	0.370	0.021
2	0.175	0.021	9	0.925	0.027	16	0.245	0.024
3	0.250	0.024	10	0.085	0.003	17	0.250	0.034
4	0.245	0.056	11	0.300	0.035	18	0.155	0.041
5	0.445	0.075	12	0.240	0.053	19	0.745	0.060
6	0.310	0.076	13	0.255	0.010	20	0.455	0.093
7	0.195	0.049	14	0.175	0.035	Mean	0.317	0.042

Noticeably, exactly the same regularity has been observed for absolutely all subjects in all experiments (see, e.g., Fig. 4 where the surface of the error values $E(\alpha, D)$ obtained for other observers is given). In other words, the parameter D_p is, in fact, the universal invariant providing the minimum E_{\min} of the error value surface $E(\alpha, D)$. Correspondingly, the quantity D_p may be treated as the intensity of the effective noise related to the individual bistable perception energy function $U(x)$. Most importantly, although we have no possibility to find quantitative characteristics of the individual perception energy function $U(x)$, we can, nevertheless, measure precisely the intensity D_p of the noise involved into the bistable visual perception. Obviously, this effective noise intensity D_p can easily be found in the experimental data with the help of the least square technique and should be considered to be in strong connection with individual particularities of the human bistable perception.

The results of the experimental studies are illustrated in Fig. 5 and summarized in Table 1, where the subject number, the obtained value of the effective noise intensity D_p , and the minimum error E_{\min} for Eq. (21) are given. As one can see for all experiments, the experimental data is in a good agreement with the theoretical curves prescribed by Eqs. (18) and (20) for which the effec-

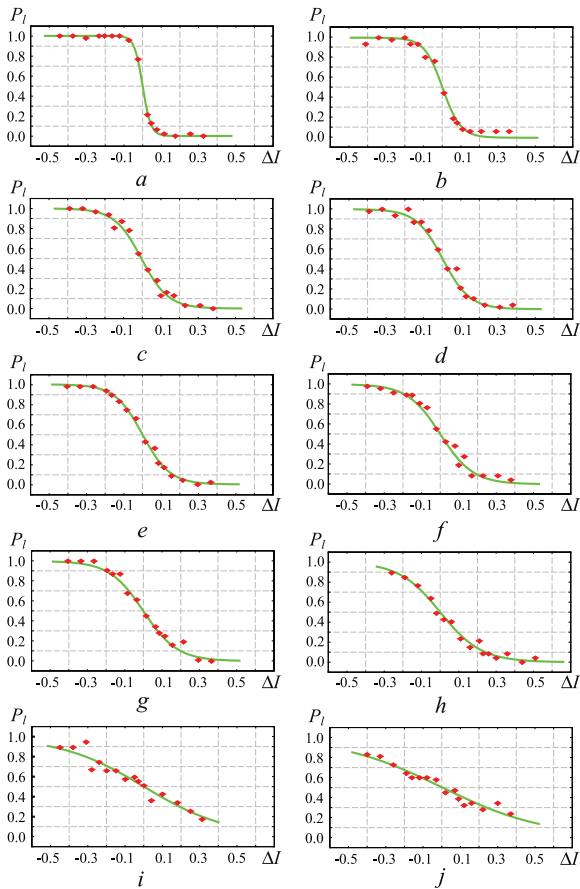


Fig. 5. Experimentally measured dependencies of the probability to perceive the left-oriented image of the Necker cube $P_l(\Delta I)$ on the asymmetry wireframe contrasts parameter ΔI obtained for ten different subjects (dots) and corresponding theoretical approximations $\hat{P}_l(\Delta I)$ shown by the solid lines. The values of the effective noise intensity D_p related to the individual bistable perception energy function are determined with the help of the least square technique. All curves are ordered by increasing effective noise intensity D_p : (a) subject #10, $D_p = 0.085$; (b) subject #14, $D_p = 0.175$; (c) subject #3, $D_p = 0.25$; (d) subject #17, $D_p = 0.25$; (e) subject #13, $D_p = 0.255$ (see also Fig. 3); (f) subject #11, $D_p = 0.3$; (g) subject #6, $D_p = 0.31$; (h) subject #15, $D_p = 0.37$; (i) subject #19, $D_p = 0.745$; (j) subject #9, $D_p = 0.925$.

tive noise intensity D_p given in Table 1 has been measured using the least square approach. We have found that the effective noise intensity D_p varies from 0.085 to 0.925 with the mean value being 0.317, the standard deviation is 0.201, and the standard error of the mean is 0.045. Remarkably, the values of E_{\min} characterizing the deviation of the experimental points $P_l(\Delta I)$ from the theoretical approximation $\hat{P}_l(\Delta I)$ are located within the interval $0.003 \leq E_{\min} \leq 0.093$ with the mean value of 0.042, standard deviation of 0.025, and standard error of the mean of 0.006.

The excellent agreement between the theoretical curves and the experimentally obtained data is the conclusive evidence of the correctness of the proposed approach aimed to quantitatively characterize the processes of the cognitive activity related to the visual perception of ambiguous images. The revealed regularity Eq. (22) is extremely important from the viewpoint of both the understanding of the brain functionality and the noise intensity measurement. The empirical character of regularity Eq. (22) in no way reduces the value of the obtained finding because absolutely all theories accepted today (whether in astronomy, physics, biology or elsewhere) are based on the preceded empirical observations. Remarkably, the examined type of the brain activity can be quantitatively characterized with the help of a single quantity, namely, the intensity of effective noise, D_p , despite individual particularities of

the human perception mechanism, as well as the lack of information about numerical parameters responsible for recognition of visual stimuli.

5. Conclusion

In this paper we have proposed a method for theoretical and experimental studies of stochastic processes in the human brain related to the perception of ambiguous images. Although all of our experiments have been performed in the morning with healthy persons, it would be very interesting to study the influence of different factors (e.g., tiredness, external disturbance, etc.) on the level of brain noise. Moreover, a study of stochastic processes in the brain of persons with cognitive difficulties and the use of the proposed technique for diagnostic and prognostic purposes seems to be an extremely important task. Obviously, the above problems require additional careful investigation.

We believe that the developed theoretical background and proposed experimental methodology will stimulate further research of cognitive brain activity involving theoreticians and experimentalists from different fields of science. The developed theory provides a solid experimentally approved basis for further understanding of brain functionality. This rather simple way to quantitatively characterize brain activity related to perception of ambiguous images will be a powerful tool, which could be used, e.g., in neurotechnology to design a brain-computer interface, and in medicine for diagnostic and prognostic purposes. We expect that our work will be interesting and useful for scientists who carry out interdisciplinary research at the cutting edge of physics, neurophysiology, psychology and medicine.

Acknowledgments

This work has been supported by the Russian Science Foundation (grant 16-12-10100).

References

- [1] Hramov AE, Koronovskii AA, Makarov VA, Pavlov AN, Sitnikova E. Wavelets in neuroscience. Springer Series in Synergetics, Springer, Heidelberg, New York, Dordrecht, London; 2015.
- [2] Bear MF, Connors BW, Paradiso MA. Neuroscience. Exploring the brain, Wolters Kluwer; 2015.
- [3] Papo D, Buldú JM, Boccaletti S, Bullmore ET. Complex network theory and the brain. Philos Trans R Soc London B 2014;369:1653. arXiv: <http://rsta.royalsocietypublishing.org/content/369/1653/20130520.full.pdf>. doi:10.1098/rsta.2013.0520.
- [4] Chavez M, Valencia M, Navarro V, Latora V, Martinerie J. Functional modularity of background activities in normal and epileptic brain networks. Phys Rev Lett 2010;104:118701.
- [5] Bick C, Rabinovich MI. Dynamical origin of the effective storage capacity in the brains working memory. Phys Rev Lett 2009;103:218101.
- [6] Wolf F. Symmetry, multistability, and long-range interactions in brain development. Phys Rev Lett 2005;95:208701.
- [7] Koronovskii AA, Hramov AE, Grubov VV, Moskalenko OI, Sitnikova E, Pavlov AN. Coexistence of intermittencies in the neuronal network of the epileptic brain. Phys Rev E 2016;93:032220. doi:10.1103/PhysRevE.93.032220.
- [8] van Luijckelaar ELM, Hramov AE, Sitnikova E, Koronovskii AA. Spike-wave discharges in WAG/Rij rats are preceded by delta and theta precursor activity in cortex and thalamus. Clin Neurophysiol 2011;122:687–95.
- [9] Hramov AE, Koronovskii AA, Midzyanovskaya IS, Sitnikova E, Rijn CM. On-off intermittency in time series of spontaneous paroxysmal activity in rats with genetic absence epilepsy. Chaos 2006;16:043111.
- [10] Schwartz J-L, Grimalt N, Hupé J-M, Moore BCJ, Pressnitzer D. Multistability in perception: binding sensory modalities, an overview. Philos Trans R Soc B 2012;367:896–905.
- [11] Cao R, Braun J, Mattia M. Stochastic accumulation by cortical columns may explain the scalar property of multistable perception. Phys Rev Lett 2014;113:098103.
- [12] Leopold DA, Logothetis NK. Multistable phenomena: changing views in perception. Trends Cognit Sci 1999;3(7):254–64.
- [13] Blake R, Logothetis NK. Visual competition, nature reviews. Neuroscience 2002;3:13–21.
- [14] Pisarchik AN, Jaimes-Reategui R, Magallón-García CDA, Castillo-Morales CO. Critical slowing down and noise-induced intermittency in bistable perception: bifurcation analysis. Biol Cybern 2014;108(4):397–404.

- [15] Pisarchik AN, Bashkirtseva IA, Ryashko LB. Controlling bistability in a stochastic perception model. *Eur Phys J Spec Top* 2015;224(8):1477–84. doi:10.1140/epjst/e2015-02473-0.
- [16] Bashkirtseva IA, LR. Stochastic sensitivity of a bistable energy model for visual perception. *Indian Journal of Physics* ((in press)).
- [17] Moore BCJ, Gockel HE. Properties of auditory stream formation. *Philos Trans R Soc B* 2012;367:919–31.
- [18] Carter O, Konkle T, Wang Q, Hayward V, Moore C. Tactile rivalry demonstrated with an ambiguous apparent-motion quartet. *Curr Biol* 2008;18:1050–4.
- [19] Zhou W, Chen D. Binaral rivalry between the nostrils and in the cortex. *Curr Biol* 2009;19:1561–5.
- [20] Etcoff NL, Magee JJ. Categorical perception of facial expressions. *Cognition* 1992;44(3):227–40. [http://dx.doi.org/10.1016/0010-0277\(92\)90002-Y](http://dx.doi.org/10.1016/0010-0277(92)90002-Y).
- [21] Liu Y, Jagadeesh B. Neural selectivity in anterior inferotemporal cortex for morphed photographic images during behavioral classification or fixation. *J Neurophysiol* 2008;100:966–82.
- [22] Freedman DJ, Riesenhuber M, Poggio T, Miller EK. Categorical representation of visual stimuli in the primate prefrontal cortex. *Science* 2001;291(5502):312–16. doi:10.1126/science.291.5502.312.
- [23] Tong F, Meng M, Blake R. Neural bases of binocular rivalry. *Trends Cognit Sci* 2006;10(11):502–11.
- [24] Sterzer P, Kleinschmidt A, Rees G. The neural bases of multistable perception. *Trends Cognit Sci* 2009;13(7):310–18.
- [25] Huguet G, Rinzel J, Hupé J-M. Noise and adaptation in multistable perception: noise drives when to switch, adaptation determines percept choice. *J Vision* 2014;14(3):1–24.
- [26] Gigante G, Mattia M, Braun J, Giudice PD. Bistable perception modeled as competing stochastic integrations at two levels. *PLoS Comput Biol* 2009;5(7):e1000430.
- [27] Moreno-Bote R, Rinzel J, Rubin N. Noise-induced alternations in an attractor network model of perceptual bistability. *J Neurophysiol* 2007;98:1125–39.
- [28] Merk I, Schnakenberg J. A stochastic model of multistable visual perception. *Biol Cybern* 2002;86:111–16.
- [29] Deco G, Rolls ET, Romo R. Stochastic dynamics as a principle of brain function. *Prog Neurobiol* 2009;88:1–16.
- [30] Kitajo K, Nozaki D, Ward LM, Yamamoto Y. Behavioral stochastic resonance within the human brain. *Phys Rev Lett* 2003;90(21):218103.
- [31] Prussek J, Lehnertz K. Stochastic qualifiers of epileptic brain dynamics. *Phys Rev Lett* 2007;98:138103.
- [32] Smith PL, Ratcliff R. Psychology and neurobiology of simple decisions. *Trends Neurosci* 2004;27(3):161–8. <http://dx.doi.org/10.1016/j.tins.2004.01.006>.
- [33] Wang X-J. Decision making in recurrent neuronal circuits. *Neuron* 2008;60(2):215–34. <http://dx.doi.org/10.1016/j.neuron.2008.09.034>.
- [34] Ratcliff R, Smith PL. A comparison of sequential sampling models for two-choice reaction time. *Psychol Rev* 2004;111(2):333–67.
- [35] Heekeren HR, Marrett S, Ungerleider LG. The neural systems that mediate human perceptual decision making. *Nat Rev Neurosci* 2008;9:467–79.
- [36] Wang X-J. Neural dynamics and circuit mechanisms of decision-making. *Curr Opin Neurobiol* 2012;22(6):1039–46. <http://dx.doi.org/10.1016/j.conb.2012.08.006>.
- [37] Pearson B, Raskevicius J, Bays PM, Pertzov Y, Husain M. Working memory retrieval as a decision process. *Journal of Vision* 14(2).
- [38] Aks DJ, Sprott JC. The role of depth and 1/f dynamics in perceiving reversible figures. *Nonlinear Dyn Psychol Life Sci* 2003;7(2):161–80.
- [39] Taed LK, Taed O, Wright JE. Determinants involved in the perception of the necker cube: an application of catastrophe theory. *Behav Sci* 1988:97–115.
- [40] World medical association. declaration of helsinki: ethical principles for medical research involving human subjects. *J Am Med Assoc* 2000;284(23):3043–5.
- [41] Necker LA. Observations on some remarkable phenomena seen in switzerland; and an optical phenomenon which occurs on viewing of a crystal or geometrical solid. *Philos Mag* 1832;3:329–43.
- [42] Leopold DA, Wilke M, Maier A, Logothetis NK. Stable perception of visually ambiguous patterns. *Nat Neurosci* 2002;5(6):605–9.
- [43] Wilson HR. Minimal physiological conditions for binocular rivalry and rivalry memory. *Vision Res* 2007;47(21):2741.
- [44] Pastukhov A, Garcia-Rodriguez PE, Haenicke J, Guillamon A, Deco G, Braun J. Multi-stable perception balances stability and sensitivity. *Front Comput Neurosci* 2013;7:17.
- [45] Carpenter RHS. Analysing the detail of saccadic reaction time distributions. *Biocybern Biomed Eng* 2012;32(2):49–63.
- [46] Gescheider GA. *Psychophysics: the fundamentals*. Lawrence Erlbaum Associates; 1997.
- [47] Wichmann FA, Hill JN. The psychometric function: I. fitting, sampling, and goodness of fit. *Percept Psychophys* 2001;63(8):1293–313. doi:10.3758/BF03194544.
- [48] Klein SA. Measuring, estimating, and understanding the psychometric function: A commentary. *Percept Psychophys* 2001;63(8):1421–55. doi:10.3758/BF03194552.
- [49] Kingdom FAA, Prins N. *Psychophysics: a practical introduction*. Academic Press; 2010.
- [50] Laing CR, Chow CC. A spiking neuron model for binocular rivalry. *J Comput Neurosci* 2002;12:39–53.
- [51] Wilson HR. Computational evidence for a rivalry hierarchy in vision. *Proc Natl Acad Sci* 2003;100:14499.
- [52] Poston T, Stewart I. *Catastrophe theory and its applications*. Pitman; 1978.
- [53] Wolberg J. *Data analysis using the method of least squares: extracting the most information from experiments*. Springer; 2005.